Development 135, 3125-3135 (2008) doi:10.1242/dev.022236

A crucial role for hnRNP K in axon development in *Xenopus laevis*

Yuanyuan Liu, Christine Gervasi and Ben G. Szaro*

We report that hnRNP K, an RNA-binding protein implicated in multiple aspects of post-transcriptional gene control, is essential for axon outgrowth in *Xenopus*. Its intracellular localization was found to be consistent with one of its known roles as an mRNA shuttling protein. In early embryos, it was primarily nuclear, whereas later it occupied both the nucleus and cytoplasm to varying degrees in different neuronal subtypes. Antisense *hnRNP K* morpholino oligonucleotides (MOs) microinjected into blastomeres suppressed hnRNP K expression from neural plate stages through to at least stage 40. Differentiating neural cells in these embryos expressed several markers for terminally differentiated neurons but failed to make axons. Rescue experiments and the use of two separate hnRNP K MOs were carried out to confirm that these effects were specifically caused by knockdown of hnRNP K expression. For insights into the involvement of hnRNP K in neuronal post-transcriptional gene control at the molecular level, we compared effects on expression of the medium neurofilament protein (NF-M), the RNA for which binds hnRNP K, with that of peripherin, another intermediate filament protein, the RNA for which does not bind hnRNP K. hnRNP K knockdown compromised *NF-M* mRNA nucleocytoplasmic export and translation, but had no effect on *peripherin*. Because eliminating NF-M from *Xenopus* axons attenuates, but does not abolish, their outgrowth, hnRNP K must target additional RNAs needed for axon development. Our study supports the idea that translation of at least a subset of RNAs involved in axon development is controlled by post-transcriptional regulatory modules that have hnRNP K as an essential element.

KEY WORDS: Cytoskeleton, Neurofilament, Peripherin, Post-transcriptional regulation, Ribonucleoprotein

INTRODUCTION

Axonal outgrowth depends on coordinating the expression of functionally interrelated genes. For example, synthesis of cytoskeletal proteins and the associated factors that regulate and organize their assembly must be matched with bouts of axonal extension to ensure that the axon is neither under- nor oversupplied. The rapidly shifting dynamics of this outgrowth makes it difficult to envision how this balance is achieved through transcriptional control alone. Placing the synthesis of cytoskeletal proteins under direct translational control would both complement transcriptional regulatory mechanisms and offer advantages to the growing axon for matching expression with demand. The dramatic shift from untranslated to translated pools undergone by the *middle neurofilament* (*NF-M*) mRNA in retinal ganglion cells during optic nerve regeneration indicates that proteins involved in building the axon are indeed under strong translational control (Ananthakrishnan et al., 2008). However, the identities of specific elements involved in the translational control of such messages and the degree to which such elements are necessary for axon outgrowth remain unresolved issues.

The life histories of mRNAs as they pass through the cell are largely governed by continually evolving sets of ribonucleoproteins (RNPs) (Moore, 2005). One idea is that RNPs may act as components of regulatory modules targeting subsets of specific functionally related messages, providing an additional level of control beyond transcription (Keene and Tenenbaum, 2002). In the nervous system, RNPs are already known to play important roles in neural plasticity and development (Perrone-Bizzozero and Bolognani, 2002; Si et al., 2003; Yao et al., 2006). Heterogeneous nuclear RNP K (hnRNP K) is the founding member of the K-homology domain family of RNPs. Although abundantly expressed in nervous system, its role there is not understood. It binds directly to the *NF-M* 3′-untranslated region (3′-UTR), along with additional RNPs, including HuB and hnRNPs E1 and E2 (Antic et al., 1999; Thyagarajan and Szaro, 2004). hnRNP K is thought to function as a central scaffolding component of evolving mRNP complexes whose compositions are modulated by multiple kinases, thereby providing a mechanism whereby mRNA fate can be coupled with cell-signaling events (Bomsztyk et al., 2004).

Two observations highlight the potential importance of the interactions of hnRNP K with neuronal mRNAs during development. In neuroblastoma cells, hnRNP K directly antagonizes Hu binding to *p21* mRNA to promote proliferation over differentiation (Yano et al., 2005). In mammalian brain, it associates with the mRNAs of three NF subunits [light (NF-L), medium (NF-M) and heavy (NF-H)] more strongly in postnatal than in adult neocortex (Thyagarajan and Szaro, 2008). To explore its role in the intact developing nervous system, we first examined the cellular distribution of hnRNP K in developing *Xenopus* and then suppressed its expression with antisense morpholino oligonucleotides (MOs) injected into blastomeres. Suppressing hnRNP K expression both blocked axonal outgrowth and inhibited the translation of NF-M. These observations are consistent with the hypothesis that hnRNP K plays an essential role in the translation of a subset of proteins involved in building the axon.

MATERIALS AND METHODS

Microinjection, rearing and culturing of embryos

Two-cell stage periodic albino *Xenopus laevis* embryos (Hoperskaya, 1975) were microinjected into one or both blastomeres (10 nl each; 1 ng/nl) with MO (Gervasi and Szaro, 2004). The following MOs (Gene Tools) were used: antisense hnRNP K MO1, 5′GCT GCT ACC TTT CTC CTA CGC CGA C3′ starting from nucleotide –54; a second, non-overlapping antisense hnRNP K MO (MO2), 5′TC TTC CTG CTC TGT CTC CAT CTT CT3′ (the initiation codon is underlined); antisense hnRNP E MO, 5′GGC TAT

The Department of Biological Sciences and the Center for Neuroscience Research, University at Albany, State University of New York, Albany, NY 12222, USA.

*Author for correspondence (e-mail: bgs86@albany.edu)

Accepted 28 July 2008

TGT CAG AAG CTG TAC AAA G3′ starting from nucleotide –50; and a standard control MO, 5′CCT CTT ACC TCA GTT ACA ATT TAT A3′. Fluorescent dextrans (FDx) were co-injected to label cells descended from the injected blastomere (0.75% w/v lysinated fluorescein-isothiocyanate Dextran; 0.1-0.25% Cascade Blue Dextran, Molecular Probes).

For rescue experiments, cDNA spanning the complete coding sequence of *X. laevis* hnRNP K (GenBank BC044711) was obtained by RT-PCR (Superscript II RT; Platinum Pfx DNA polymerase, Invitrogen) from total RNA of stage 29/30 embryos using the following primers, which had *Not*I sites added to their 5′-end to facilitate cloning: 5′ATA GCG GCC GCT AAA AGA AGA TGG AGA CAG AGC AGG3′ (forward); and 5′ATA GCG GCC GCG AAG TCA AAA CCC ATA AGA ATA ATC3′ (reverse). PCR products were ligated into the *Not*I site of a modified pGem3Z expression vector (pSP6-XhnRNPK), downstream of the SP6 promoter and upstream of the 3′ UTR of rabbit β-globin (Lin and Szaro, 1996). The insert sequence was confirmed to match the GenBank sequence. The plasmid was subsequently linearized with *Xho*I for use as template for in vitro transcription of 5′-capped RNA (mMESSAGE mMACHINE SP6, Ambion). Rescue was performed by co-injecting two-cell embryos with hnRNP K-MO1 (10 ng) plus hnRNP K RNA (50-1000 pg).

Dissociated embryonic spinal cord-myotomal cultures were prepared from spinal cord, including extreme caudal hindbrain together with surrounding myotomes, of stage 22 embryos. Each culture was prepared from a single embryo and grown at 22.5°C on 35 mm polystyrene dishes (Δ plastic, Nunclon Nalge International), as described (Tabti and Poo, 1991; Undamatla and Szaro, 2001).

Immunohistochemical staining and western blots

The following antibodies were used (#1-7, mouse monoclonal; #8, rabbit antiserum): (1) *Xenopus* NF-M, 2 μg/ml [RMO270 (Szaro et al., 1989; Wetzel et al., 1989)]; (2) a neuronal β-tubulin isotype, 1:100 [JDR.38B, Sigma (Moody et al., 1996)]; (3) hnRNP K, 1:100 (Santa Cruz Biotechnology); (4) HNK-1, undiluted hybridoma supernatant (Nordlander, 1989; Szaro et al., 1991); (5) a phosphorylated epitope of the C-terminal tail domain of *Xenopus* NF-M, 1:200 [S6 (Szaro and Gainer, 1988)]; (6) *Xenopus* MAP-1, 1:200 [8D-12 (Lin and Szaro, 1996)]; (7) glyceraldehyde phosphate dehydrogenase (GAPDH), 5 μg/ml (clone 6C5, Ambion); and (8) *Xenopus* peripherin, 1:2000 (Gervasi et al., 2000). Alexa Fluor phalloidin 555 and DAPI (Molecular Probes) were used at 25 μl/ml and 300 nM to stain F-actin filaments and nuclei, respectively.

The numbers of embryos injected with each MO and analyzed in whole-mount are presented in Table 1. For whole-mount immunohistochemistry, embryos were fixed in phosphate-buffered (0.1 M sodium phosphate, pH 7.4) 10% formalin and processed as described, using biotinylated secondary antibodies and fluorescent avidins (Dent et al., 1989; Gervasi et al., 2000). Fluorescence was quantified from confocal microscope images using Metamorph software (version 4.5.6, Molecular Devices). For frozen sections (12 μm transverse), juvenile frogs were anesthetized, perfusion fixed with paraformadehyde, and processed for immunoperoxidase staining using diaminobenzidine with nickel chloride as the chromogen (Szaro and Gainer, 1988). For dissociated cell cultures, cells were fixed 24 hours after plating for 2 hours in phosphate-buffered 1% formaldehyde/2% sucrose at room temperature and processed for immunofluorescence procedures using biotinylated secondary antibodies and rhodamine-avidin (Undamatla and Szaro, 2001). For phalloidin staining, cultures were fixed in phosphate-buffered 4% paraformaldehyde/2% sucrose and processed as described (Smith et al., 2006).

For western blots, 60-80 stage 29/30 embryos per sample were homogenized in SDS-urea sample buffer, of which 45 μg protein per lane was separated by 7.5% SDS-PAGE, transferred overnight (60V, 12°C) to nitrocellulose, and processed for immunoperoxidase staining (Zhao and Szaro, 1994). Blots were processed separately with primary antibodies to either hnRNP K or NF-M then stripped and reprocessed for GAPDH. Staining was visualized by chemiluminescence (SuperSignal West Pico; Pierce) and imaged on a ChemiDoc XRS System (Biorad, Hercules, CA). Band intensities were quantified using Quantity One software (Biorad).

In situ hybridization

Digoxigenin-labeled cRNA probes were transcribed using a Genius 4 Kit (Roche) from plasmids containing *Xenopus peripherin* (2.0 kb) and *NF-M* cDNAs (clone 6B-1a of NF-M1, 1.7 kb) (Gervasi et al., 2003). *Peripherin* sense cRNA was used to control for non-specific hybridization. Whole-mount in situ hybridization was performed on stage 37/38 tadpoles (Shain and Zuber, 1996): hybridization, 18 hours at 60°C; probe concentration, 1-2 mg/ml; high stringency washes (50% formamide/2×SSC at 60°C for 30 minutes). Anti-digoxigenin Fab fragments coupled to alkaline phosphatase were used to visualize staining (Genius 3 Kit; Roche). Fluorescence in situ hybridization (FISH) was performed using the above probes, hybridization and wash conditions, followed by immunohistochemistry with peroxidase-conjugated anti-digoxigenin and tyramide-FITC (Davidson and Keller, 1999). For combined FISH-immunohistochemistry, preparations were processed for FISH first, then for rhodamine-conjugated immunofluorescence and finally for DAPI staining.

Co-immunoprecipitation of RNPs and RNAs

Co-immunoprecipitation (co-IP) of hnRNP K and RNAs was carried out on samples from juvenile frog brain using protein A-sepharose beads (CL4B, Sigma) coated with purified monoclonal antibodies to hnRNP K (clone 3C2; Santa Cruz Biotechnology) or β-galactosidase (Z3783; Promega) (Tenenbaum et al., 2002; Thyagarajan and Szaro, 2008). Prior to IP, 10% of the sample was used (total input control, TIC) to ascertain mRNA levels in the original sample. For reverse transcriptase polymerase chain reaction (RT-PCR), the primers for the first round of PCR (30 cycles of 95°C for 1 minute; 55°C for 30 seconds; 72°C for 1 minute) were as follows (sense and antisense, respectively): *NF-M*, 5′ATT CAG AGG AGC AAA AGG AT3′ and 5′TCC TGC TGC TTG CTG CAA TT3′; *peripherin*, 5′TTC ATG AGG AGG AAC TCA AT3′ and 5′TCC TCC GAC TCT TGT ACG TT3′; *EF-1α*, 5′ACC CTG CTG GAA GCT CTT GA3′ and 5′ GCA GAC GGA GAG GCT TAT CAG T3′. For the second round of amplification for *peripherin* (15 additional cycles: 95°C for 1 minute; 55°C for 30 seconds; 72°C for 1 minute), 5 μl of the first reaction and a second, nested set of *peripherin* primers was used: 5′GGT CCG CTA CCT GGA GCA GC3′ and 5′ACA TTG AGC AGG TCT TGG TA3′. PCR products were visualized on a 1% agarose-TBE gel stained with ethidium bromide.

Polysomal profiling

Embryos were collected at stages 25 and 29/30 (5 embryos per sample) and processed for polysomal profiling by ultracentrifugation on a 5-56% linear sucrose gradient (Meyuhas et al., 1996; Ananthakrishnan et al., 2008). Cellular nuclei were first separated from the cytosol by centrifugation (285 ***g***, 4°C, 2 minutes). To quantify nuclear and cytosolic *peripherin* and *NF-M* mRNA, total RNA was isolated from the nuclear pellet and from 10% of the cytosolic fraction (RNeasy Micro Kit, Qiagen). The remainder of the cytosol was used for polysome profiling. For each fraction, a spectrophotometric reading for total RNA (2 μl, A_{260}; NanoDrop

Table 1. Numbers of embryos processed for immunohistochemistry and in situ hybridization

	Staining						
Treatment	hnRNP K	NF-M protein	NF-M mRNA	Peripherin protein	Peripherin mRNA	Neuronal β-tubulin	HNK-1
hnRNP K MO1	215	183	67	192	46	157	33
hnRNP K MO2	173	126	n/a	52	n/a	46	n/a
Control MO	196	164	25	143	19	107	28
Dye alone	119	86	11	22	n/a	21	14
Uninjected control	186	108	24	102	21	93	21
hnRNPK MO1+mRNA	60	55	n/a	n/a	n/a	31	n/a

Technologies) was taken, and *peripherin* and *NF-M* mRNA levels were quantified from the remainder by quantitative real-time RT-PCR (qRT-PCR; Applied Biosystems, ABI SDS 7900HT; ABI SDS software, version 2). The following primers were used (forward and reverse): *NF-M*, 5′ACC GAA GAA GTC TTC AGG AAT AGG TA3′ and 5′CAC TGT CCG GCT CAT GCA3′; *peripherin*, 5′GCT GTA AGC GAC TTT GGT GCT A3′ and 5′CAA GGC ATG ATG GGA CAG AGT3′. Taqman probes were as follows: *NF-M*, 5′-6FAM CTG ACC GAG GCT GCA GA MGBNFQ-3′; *peripherin*: 5′-6FAM CAT TCC CTG CCT CTG TGT ATT GGC TGG TAMRA-3′.

RESULTS

Developmental expression pattern of hnRNP K

Previous biochemical studies had shown that hnRNP K in *Xenopus* is initially expressed as a maternal protein in oocytes and is present throughout early development, with expression increasing as cells differentiate (Marcu et al., 2001; Iwasaki et al., 2008). Results from whole-mount immunocytochemistry were consistent with these earlier biochemical studies and further found that hnRNP K was present in all the germ layers from blastulae stages onwards (illustrated at stages 10, 15, 22, 37 and 42 in Fig. 1). Throughout development, hnRNP K was prominently expressed in nuclei. From gastrula stages onwards, hnRNP K became progressively more highly expressed in ectodermal and mesodermal derivatives, such as neural plate and somites, than in endodermal ones. This trend continued through early tadpole stages, where hnRNP K staining in differentiating tissues, especially in nervous system, became increasingly more cytoplasmic (Fig. 1F).

To improve resolution of intracellular structures, we next examined hnRNP K expression in dissociated embryonic spinal cord-myotomal co-cultures. At 24 hours after plating, hnRNP K immunostaining colocalized with DAPI-stained nuclei in both neurons and muscle cells (Fig. 2A-C); it was detectable neither in neurites nor in growth cones (Fig. 2C). In histological sections of post-metamorphic frog nervous system (Fig. 2D,E), the relative intensity of nuclear versus cytoplasmic staining varied extensively among cell populations. In retinal ganglion cells, for example, immunostaining was generally more intense in cytoplasm than in nuclei (Fig. 2D), and in spinal cord motoneurons, intensities of cytoplasmic when compared with nuclear staining were more comparable (Fig. 2E). Nuclear versus cytoplasmic staining varied considerably among other brain and spinal cord cell types, with numerous examples of cells having greater nuclear than cytoplasmic staining, and vice versa. These data are consistent with the idea that hnRNP K shuttles between the nucleus and cytoplasm, escorting its RNA targets to assist their recruitment into mRNP granules and ribosomes (Piñol-Roma and Dreyfuss, 1992; Moore, 2005). hnRNP K immunostaining was not found in axons (e.g. optic nerve and ventral spinal cord white matter; see Fig. S1 in the supplementary material), indicating that hnRNP K is unlikely to play a major role in axonal transport of mRNAs.

Suppression of hnRNP K expression with antisense morpholino oligonucleotides

To study its function during development, we suppressed hnRNP K expression with antisense MOs. The bilateral symmetry of the embryo enabled the application of anatomical criteria to identify affected cellular subtypes in unilaterally injected embryos; FDx was co-injected to identify the injected side. To control for inadvertantly targeting genes other than hnRNP K, we injected two separate *hnRNP K* antisense MOs targeting non-overlapping regions of the 5′-UTR (Heasman, 2002). As an additional control, we injected a third MO targeting the 5′-UTR of *Xenopus hnRNP E* (Gravina et al., 2002), the closest relative of *hnRNP K* (Ostareck-Lederer et al., 1998). A standard control MO was added to control for non-specific MO effects.

Up to gastrula stages, neither *hnRNP K* MO had any discernible effect on hnRNP K expression (Fig. 3A1,A2). This was most likely because of a large store of maternal protein (Iwasaki et al., 2008). By neural plate stages, however, expression was strongly suppressed throughout the injected half of the embryo (Fig. 3B1,B2). The efficacies of the two *hnRNP K* MOs at suppressing hnRNP K expression were similar and the resulting phenotypes (described later) were indistinguishable. Neither *hnRNP K* MO had any effect on *hnRNP E* expression (not shown), nor did the *hnRNP E* and standard control MOs have any effect on hnRNP K (see Fig. S2 in the supplementary material). Suppression of hnRNP K expression persisted through at least stage 40 (Fig. 3C-E). The suppression of hnRNP K was also assessed by western blots of stage 29/30 embryos (see Fig. S3 in the supplementary material). Neither unilateral nor bilateral injections of hnRNP K MO1 had any effect on GAPDH expression. Embryos receiving control MO expressed 97±5% (s.d.) (three blots) as much hnRNP K as uninjected ones, and embryos receiving unilateral or bilateral injections of hnRNP K MO1 expressed 57±6% and 8±3%, respectively, as much as uninjected ones.

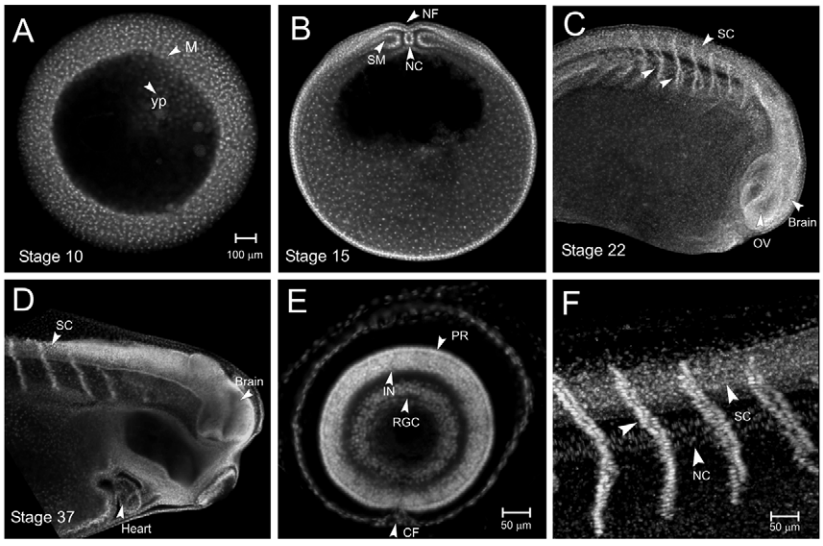

Fig. 1. Expression of hnRNP K in whole-mount embryos. (**A**) Stage 10 gastrula; hnRNP K was found in all germ layers, but was most intense in mesectoderm (M). yp, yolk plug. (**B**) Stage 15 neural plate; hnRNP K staining intensified in mesectoderm. NF, neural plate and adjacent neural folds; NC, notochord; SM, somitic mesoderm. (**C-F**) Stage 22 tailbud (C), stage 37/38 tadpole (D), stage 42 tadpole (E,F). hnRNP K was abundant in brain and spinal cord (SC), in aligned nuclei of somitic muscle (unlabeled arrowheads) and all retinal layers by stage 42 (E). OV, optic vesicle; RGC, retinal ganglion cell layer; IN, interneuron layer; PR, photoreceptor layer; CF, choroidal fissure. NC, notochord. Scale bars: in A, 100 μm for A-D; 50 μm in E,F.

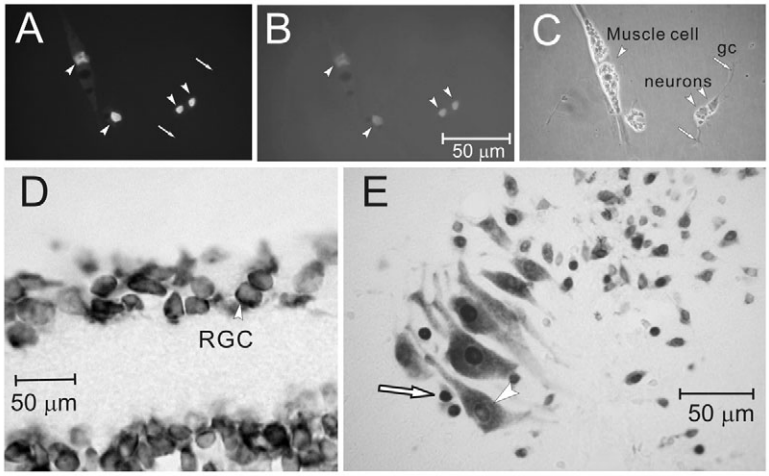

Fig. 2. Transition of hnRNP K from predominantly nuclear to mixed nuclear and cytoplasmic localization during neuronal development. (**A-C**) hnRNP K immunofluorescence (A), DAPI-fluorescence (B) and phase-contrast (C) images of embryonic muscle cell and neurons in dissociated cell culture. hnRNP K immunostaining colocalized with DAPI-stained nuclei (arrowheads, A,B); neurites and growth cones (gc) had no immunostaining (arrows in A,C). (**D**,**E**) hnRNP K immunoperoxidase staining of sections of juvenile frog retina (D) and spinal cord ventral horn (E). Retinal ganglion cells (RGC) exhibited more intense cytoplasmic than nuclear staining; motoneuron staining was both in the nucleus and cytoplasm (arrowhead, E). Arrow in E indicates interneuron with predominantly nuclear staining.

Effects of hnRNP K knockdown on development of intact embryos

By external criteria, *hnRNP K* MO-injected embryos developed normally through stage 20. At stage 22, the injected sides of hnRNP K MO-injected animals began to constrict, leading to a 'bent' phenotype. Despite this bending and additional mild defects in anterior cranial and optic vesicle formation, rates of survival through stage 40 (assayed in 19 spawnings) were indistinguishable between *hnRNP K* MO-injected embryos and controls: hnRNP K MO1, 91±4% of 2042 embryos; hnRNP K MO2, 92±3% of 1039; control MO, 94±5% of 1739; FDx alone, 93±6% of 1106; and uninjected embryos, 94±4% of 2598. None of these survival rates differed significantly (P>0.1, one-way ANOVA).

We next examined effects of hnRNP K knockdown in neurons by whole-mount immunostaining of tadpoles (stage 37/38) for several neuronal antigens typically found in both perikarya and axons. In all cases, phenotypes obtained with either of the two *hnRNP K MO*s were indistinguishable. We first looked at a phosphorylation-independent epitope of NF-M (RMO270). In contrast to uninjected and control MO-injected animals (Fig. 4A), NF-M immunostaining of optic (not shown), motor and sensory nerves was severely compromised on the *hnRNP K* MO-injected side (MO1, Fig. 4B: MO2, Fig. 4C). Rostrocaudal spinal tracts on the injected side were also stained less intensely than on the uninjected side (separated by the broken line, Fig. 4B,C). Because these tracts contain decussated axons, we believe that such staining on the injected side may have originated from the uninjected side. The absence of any NF-M immunostained perikarya on the injected side supported this possibility and further indicated that NF-M protein expression was also likely to have been affected. Western blots of stage 29/30 embryos were used to confirm this suppression (see Fig. S3 in the supplementary material). Whereas control MO-injected animals expressed 88±7% (±s.d.) (three blots) as much NF-M as uninjected ones, animals unilaterally and bilaterally injected with hnRNP K MO1 expressed only 56±4% and 9±4% as much, respectively.

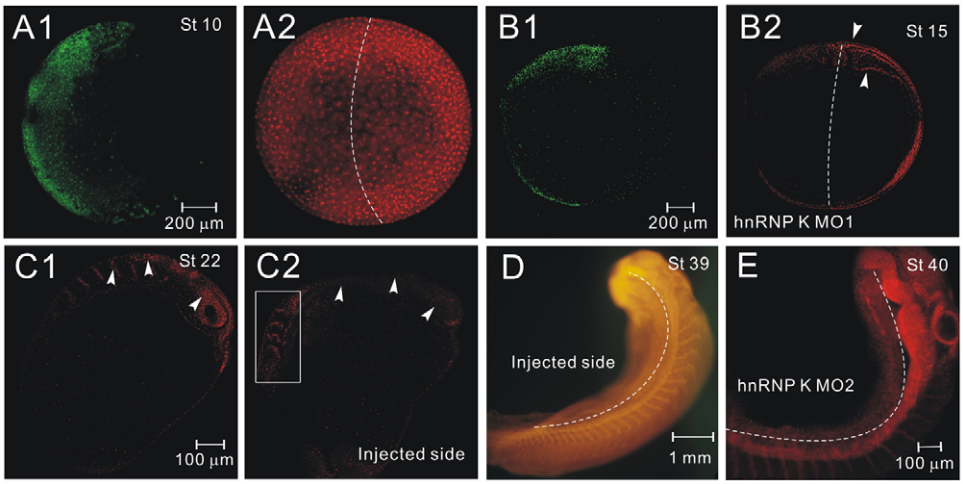

Fig. 3. Suppression of hnRNP K expression by antisense MO. Embryos were unilaterally injected with two separate non-overlapping hnRNP K MOs (MO1 in A-D; MO2 in E). (**A1**,**A2**) Stage 10 gastrula; persistent maternal hnRNP K expression. (**B1**,**B2**) Stage 15 neural plate stage; suppression of hnRNP K expression on the injected side (left of broken line). Upper arrowhead, neural fold; lower arrowhead, somitic mesoderm, on the uninjected side. (**C1**,**C2**) Stage 22 tailbud stage; hnRNP K expression in myotome, spinal cord and brain (arrowheads, left to right, respectively) was suppressed on the injected side (C2) when compared with the uninjected side (C1). Because the animals are bent, the optical section in C2 also contained some cells from the uninjected side of the embryo (rectangle). (**D**,**E**) Three-day tadpole (stages 39 and 40); the uninjected side exhibited normal staining and morphology, but the injected side exhibited only background immunostaining and some defects in somites. (A1-C2,E) Confocal optical sections; (D) fluorescence dissecting microscopic view of whole animal. hnRNP K immunostaining, red; co-injected FITC-dextran, green.

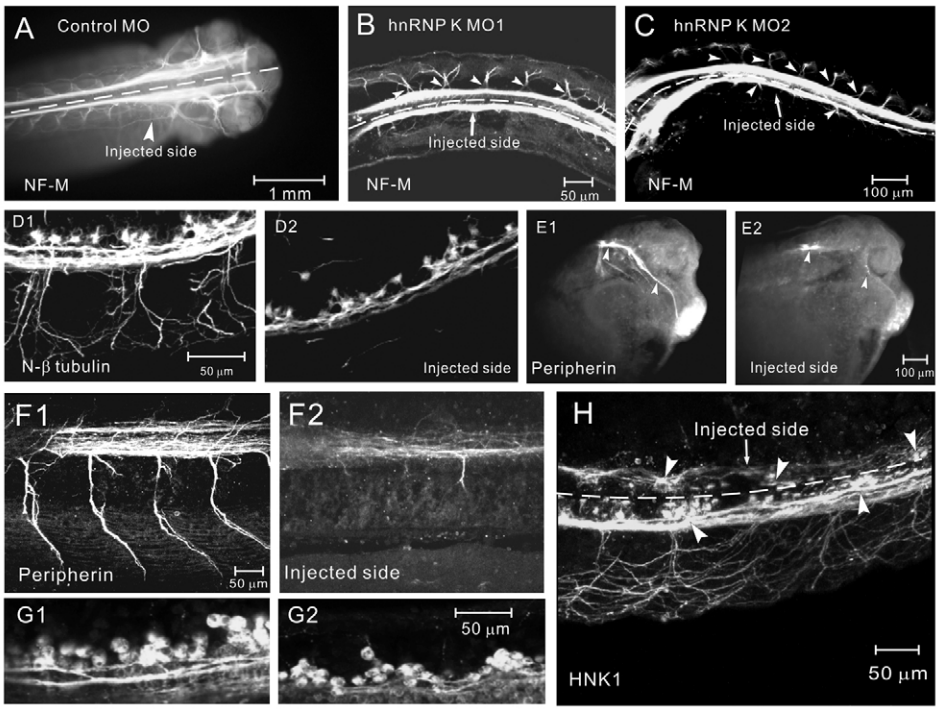

Fig. 4. Suppression of axonal outgrowth by hnRNP K MO in intact animals. Embryos unilaterally injected with control MO (A), hnRNP K MO1 (B,D-H) or hnRNP K MO2 (C) processed at stage 37/38 by whole-mount immunofluorescence. (**A-C**) Embryos injected with control MO (A), hnRNP K MO1 (B) or MO2 (C), and immunostained for NF-M. Broken lines separate injected (lower) from uninjected (upper) sides. (B,C) Arrowheads on the injected side indicate peripheral motor axons; arrowheads on the uninjected side indicate residual wispy peripheral axons. (A) View under the fluorescence dissecting microscope; (B,C) stacked confocal optical sections. (**D1**) Neuronal β-tubulin staining in neuronal perikarya and peripheral axons of spinal cord, uninjected side. (**D2**) Tubulin staining in perikarya and a few scattered fibers, injected side. (**E1-G2**) Peripherin immunostaining of head (E1,E2) and spinal cord (F1,F2,G1,G2). (E1,F1,G1) Uninjected side; (E2,F2,G2) injected side. (E1,E2) Trigeminal ganglion neuronal perikarya (upper arrowhead) and nerves (lower arrowhead). (F1,F2) Spinal cord with peripheral motor axons. (G1,G2) Spinal cord neuronal perikarya. (**H**) Spinal cord immunostained for HNK-1. Robust staining of neuronal perikarya and axons on the uninjected side (below the broken line); clusters of stained neuronal perikarya (arrowheads) and very few fibers on the injected side (above the broken line). Scale bars in D1,E2,F1 and G2 also apply to D2,E1,F2 and G1, respectively.

As the absence of NF-M stained axons might therefore have been due to the suppression of NF-M expression, we next stained animals for three additional neuronally expressed antigens normally present in neuronal perikarya and axons (Fig. 4D1-H). Two of these were cytoskeletal proteins, neuronal β-tubulin (visualized with antibody JDR.38B) and peripherin (visualized with a rabbit antiserum). These proteins are abundant in all developing *Xenopus* axons from the time of neurite initiation onwards (Moody et al., 1996; Gervasi et al., 2000; Undamatla and Szaro, 2001). The HNK-1 antibody targets an extracellular carbohydrate moiety, and in *Xenopus* developing spinal cord, it stains terminally differentiated neurons and their axons (Nordlander, 1989). On the uninjected side, all three exhibited patterns of staining that are typical for these antibodies: i.e. clusters of cell bodies in spinal cord and peripheral ganglia, as well as robustly stained CNS axon tracts, motor axons and peripheral sensory axons. On the injected side, clusters of neuronal perikarya were well stained, indicating that the hnRNP K MO had little effect on their overall expression. This conclusion was confirmed by comparing the relative intensities of peripherin immunofluorescence quantitatively from confocal microscopic images. On the injected side, the mean pixel intensity per cell was 95% that of the uninjected side [142±33 (s.d.) in 120 cells versus 150±26 in 114 cells, respectively]. Thus, the absence of axons cannot reasonably be attributed to faint immunostaining. On the *hnRNP K* MO-injected side, spinal cord CNS tracts were only very lightly stained, and only a very few short wispy peripheral axons were seen emanating from spinal cord and cranial ganglia. In all control MO-injected cases, staining with these antibodies was bilaterally symmetric and indistinguishable from that of uninjected animals. The incidence of these effects is summarized in Table 2. Because staining with three independent markers failed to reveal axons but was unaffected in perikarya, we concluded that hnRNP K knockdown compromised axonal outgrowth but not neuronal determination.

Rescue of effects on axon outgrowth and NF-M expression by co-injection of hnRNP K RNA

To confirm that effects on axon outgrowth and NF-M expression were specific to *hnRNP K*, we co-injected in vitro transcribed *Xenopus hnRNP K* RNA lacking the MO targeting site (50-1000 pg) plus hnRNP K MO1 (10 ng). Injection of 1000 pg of RNA proved lethal (33 embryos), but at 100 and 250 pg per embryo, hnRNP K expression was largely restored (30 embryos each). Co-injected animals continued to bend towards the injected side to varying degrees among animals, but less so than in animals receiving hnRNP K MO alone, providing external confirmation of partial rescue. hnRNP K immunostaining intensity on the injected side also varied among animals but was generally distributed as in normals (Fig. 5A). For example, hnRNP K immunostaining on the injected side appeared in somitic myocyte nuclei, although myotomes were generally smaller and nuclei were less well aligned than normal.

Table 2. Incidence of axonal defects in unilaterally injected intact embryos*

Markers for axon staining	Morpholino	Severe axon outgrowth defects	Slight to moderate axon outgrowth defects	Normal axon outgrowth	*n*
NF-M	MO1	175	8	0	183
	MO2	116	10	0	126
	CM	0	3	161	164
	MO1+RNA	5	45	5	55
Peripherin	MO1	176	16	0	192
	MO2	47	4	1	52
	CM	0	4	139	143
Neuronal β-tubulin	MO1	149	8	0	157
	MO2	42	4	0	46
	CM	1	3	103	107
	MO1+RNA	3	25	3	31
HNK-1	MO1	32	1	0	33
	CM	0	0	28	28

*Embryos were unilaterally injected at the two-cell stage and assayed at stage 37/38 by whole-mount immunostaining. Severe defects include virtually no peripheral axonal outgrowth on the injected side, except for a few wispy fibers. Slight to moderate defects include axons formed, but with visibly less robust outgrowth or staining intensity.
CM, control MO.

Next, embryos co-injected with hnRNP K MO and 100-250 pg of RNA were immunostained in whole mount for neuronal β-tubulin and NF-M. Both peripheral axon outgrowth and NF-M expression were effectively restored (Table 2; Fig. 5B,C), with the degree of restoration inversely correlating with the severity of the 'bent' phenotype. Thus, MO effects on axon outgrowth and NF-M protein expression can be attributed to the suppression of hnRNP K expression.

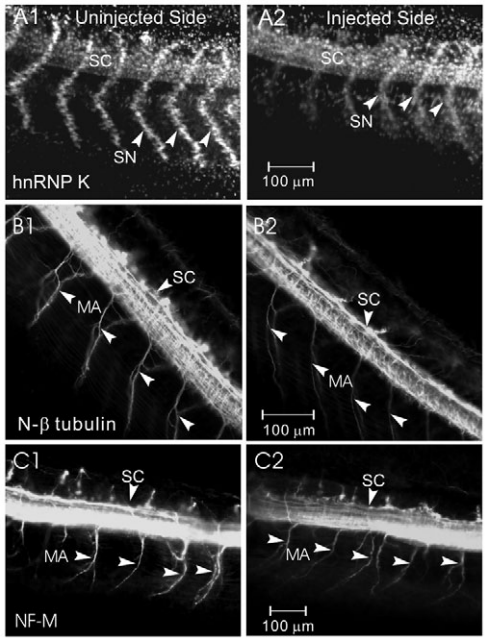

Fig. 5. Rescue from hnRNP K MO by co-injection of hnRNP K RNA. Two-cell embryos were unilaterally injected with hnRNP K MO1 plus 100 pg of hnRNP K RNA, then processed for whole-mount immunostaining for hnRNP K (**A1**,**A2**), neuronal β-tubulin (**B1**,**B2**) or NF-M (**C1**,**C2**). Images are stacks of five confocal microscopic optical sections taken from the uninjected (A1,B1,C1) and injected (A2,B2,C2) sides of the same animal, parasagitally through the spinal cord. SC, spinal cord; MA, motor axons; SN, cellular nuclei of somitic myotomes. Scale bars in A2,B2,C2 also apply to A1,B1,C1, respectively.

Endogenous association of hnRNP K with NF-M but not peripherin mRNA

hnRNP K has been implicated in multiple aspects of post-transcriptional regulation (Bomsztyk et al., 2004). To gain insights into its specific role in post-transcriptional gene expression, we examined effects of hnRNP K knockdown on NF-M expression, a known target of hnRNP K. We compared these effects with those on peripherin, a functionally similar protein whose RNA is not a target. NF-M is a Type IV and peripherin is a Type III neuronal intermediate filament protein. Although both are found together in developing axons, peripherin is generally expressed earlier than NF-M, and thus their expressions are separately controlled (Gervasi et al., 2000).

hnRNP K has been shown in vitro in both *Xenopus* and rat to bind directly to the *NF-M* 3′-UTR, but, as of yet, this interaction has only been demonstrated to occur endogenously in rat (Thyagarajan and Szaro, 2004; 2008). To confirm an endogenous association in *Xenopus*, hnRNP K-containing RNP-RNA complexes extracted from juvenile frog brain were co-immunoprecipitated with anti-hnRNP K, then assayed by RT-PCR and agarose gel electrophoresis for *NF-M* (Fig. 6A). Co-IP *NF-M* PCR product was readily visible and enriched (lane 3) over pre-IP product (TIC, lane 2). Product was missing from IPs performed with purified anti-β-galactosidase monoclonal antibody (lane 4), confirming the specificity of the hnRNP K antibody. *Xenopus EF-1α*, which is not an hnRNP K target (lane 5), was also missing from the anti-hnRNP K co-IP, confirming the specificity of the interaction with *NF-M* mRNA. No *peripherin* RT-PCR product was detected in the hnRNP K-IP, even after two rounds of amplification with nested sets of primers (Fig. 6B; lanes 4 and 5). Thus, in *Xenopus* brain, *NF-M* mRNA associates endogenously with hnRNP K but *peripherin* mRNA does not.

Effects of hnRNP K suppression on mRNA expression of NF-M and peripherin

Unilaterally injected *hnRNP K* MO tadpoles (stage 39/40) expressed *NF-M* mRNA in neuronal perikarya on both sides (Fig. 6C), indicating that the loss of NF-M protein expression was not due primarily to transcriptional effects. Although in some instances *NF-M* mRNA staining was less intense on the injected side, this was not always the case (Fig. 6D, seen with FISH). Because, in dissociated cell culture, NF-M expression increases

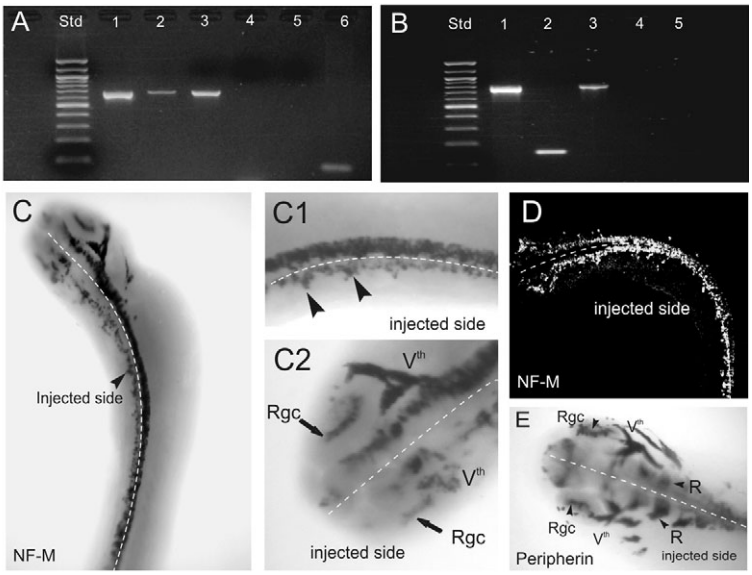

Fig. 6. Binding to hnRNP K and expression of NF-M mRNA in vivo. (**A**,**B**) Co-immunoprecipitation and RT-PCR of NF-M (A) and peripherin (B) mRNAs with hnRNP K from juvenile brain. (1) *NF-M* PCR from plasmid template with *Xenopus NF-M* cDNA insert, which served as a positive control for *NF-M* PCR amplification. (2) *NF-M* RT-PCR of sample prior to co-IP, demonstrating *NF-M* mRNA presence in the lysate. (3) *NF-M* RT-PCR of anti-hnRNP K co-IP. (4) *NF-M* RT-PCR of anti-β-galactosidase co-IP, a control for non-specific IP. (5) *EF1-α* RT-PCR of hnRNP K co-IP, demonstrating absence of mRNAs not associating with hnRNP K. (6) *EF1-α* RT-PCR of TIC, demonstrating its presence in lysate. (B) (1,2) *peripherin* PCR from plasmid template, which served as positive controls for *peripherin* PCR with each primer set. (3) *peripherin* RT-PCR of lysate prior to co-IP using the first pair of primers (30 cycles). (4,5) *peripherin* RT-PCR of anti-hnRNP K co-IP with the first (30 cycles) and second (15 additional cycles) pair of nested primers, respectively. Std, 1 kb DNA ladder (NE Biolabs). (**C-E**) Expression of *NF-M* and *peripherin* mRNAs in unilaterally injected hnRNP K MO animals. Dorsal views in whole mount of the entire animal (C), spinal cord (C1) and head (C2) of a stage 39/40 tadpole, processed for *NF-M* in situ hybridization (digoxigenin-alkaline phosphatase). Stained neurons are on both sides of the spinal cord (C; arrowheads in C1) as well as in brain, trigeminal ganglion (Vth) and retinal ganglion cells (Rgc, C2). (D) Horizontal confocal optical section of a unilaterally injected stage 39/40 *hnRNP K* MO tadpole processed for *NF-M* FISH. Rostral is towards the upper left. (E) Dorsal view of the head of a stage 39/40 *hnRNP K* MO tadpole stained for *peripherin* mRNA. R, rhombomeres.

when spinal neurites contact muscle (Undamatla and Szaro, 2001), this reduction was possibly due to the loss of such contacts. *Peripherin* mRNA was robustly and equivalently expressed on both sides of hnRNP K-knockdown animals (Fig. 6E), indicating that hnRNP K knockdown did not lead to generalized reductions in transcriptional activity.

Effects of hnRNP K knockdown on neuronal development in dissociated cell culture

Dissociated embryonic spinal cord-myotome cell cultures were used to determine whether the effects on axon outgrowth seen in intact embryos were cell-autonomous and to provide independent confirmation of the antibody staining in whole mount that axon outgrowth is compromised; in culture, it is readily seen under phase-contrast illumination without immunostaining. Suppression of hnRNP K expression was as effective in culture as in whole mount, persisting through 2 days of culture (corresponding to 3 days of development, not illustrated). Only a few cells descended from *hnRNP K* MO-injected blastomeres (identified by FDx) retained any residual, albeit barely detectable, hnRNP K 24 hours after plating: 3±2% (mean of four dishes) of FDx-labeled cells for *hnRNP K* MO-injected cultures when compared with 87±3% (mean of three dishes) of FDx-labeled cells for control MO-injected cultures (significant at $P<0.01$, *t*-test). Conversely, hnRNP K immunostaining in control MO cultures was comparable with uninjected cultures.

To assay whether hnRNP K knockdown compromised neuronal determination and survival rates in culture, two markers for neurons were used: immunostaining for neuronal β-tubulin and FISH for *NF-M*. Embryos were bilaterally injected to ensure that all cells were descended from injected blastomeres. As identified by neuronal β-tubulin immunostaining, the numbers of 'neurons' per dish were (±s.e.m., four dishes at 24 hours): *hnRNP K* MO-injected, 245±17; control MO-injected, 269±17; uninjected, 287±16. Comparable data were obtained when *NF-M* FISH was used to label neurons (four dishes): *hnRNP K* MO-bilaterally injected, 234±20; *hnRNP K* MO-unilaterally injected, 256±16; control MO-injected, 290±12; uninjected cultures, 261±13. In no case did counts differ significantly ($P>0.1$, one-way ANOVA).

Using *NF-M* FISH to identify neurons, we quantified neurite outgrowth (Fig. 7) under phase-contrast illumination (Fig. 7A,B). The percentages of 'neurons' with one or more neurites were indistinguishable between uninjected and control MO-cultures (Fig. 7C). As might be expected, unilaterally injected *hnRNP K* MO cultures had approximately half as many neurite-bearing 'neurons' as uninjected and control MO-cultures, whereas bilaterally injected *hnRNP K* MO cultures had virtually none (~2%). These differences were statistically significant ($P<0.01$, one-way ANOVA), thus confirming that the effects on axon outgrowth are cell autonomous. In addition, as reported in chick spinal cord (Bennett and DiLullo, 1985), control cultures had the occasional cell expressing NF-M protein (Fig. 7D-E′) but lacking neurites, indicating that having a neurite is not a necessary precondition for NF-M protein expression. In addition, because cells lacked even early signs of neurite initiation, we concluded that inhibition of outgrowth began as early as axon initiation.

Effects of hnRNP K knockdown on intracellular localization of NF-M mRNA

Because hnRNP K has been implicated in shuttling RNAs from the nucleus (Bomsztyk et al., 1997; Bomsztyk et al., 2004; Mikula et al., 2006), we used FISH to localize *NF-M* RNA intracellularly during hnRNP K knockdown. In whole mount, on the uninjected side of *hnRNP K* MO tadpoles, spinal cord neuronal nuclei were better defined by circumferential cytoplasmic FISH-staining than were those on the injected side (Fig. 8A,A′). For better resolution of this phenomenon, we performed NF-M double FISH-immunohistochemistry in culture. In control cultures, NF-M protein extended into neurites and the RNA surrounded the nucleus (labeled with DAPI), as is normal (Fig. 8B1-3). In unilaterally injected *hnRNP K* MO-cultures, such 'normal' neurons could be seen adjacent to cells that were unstained for NF-M protein and had

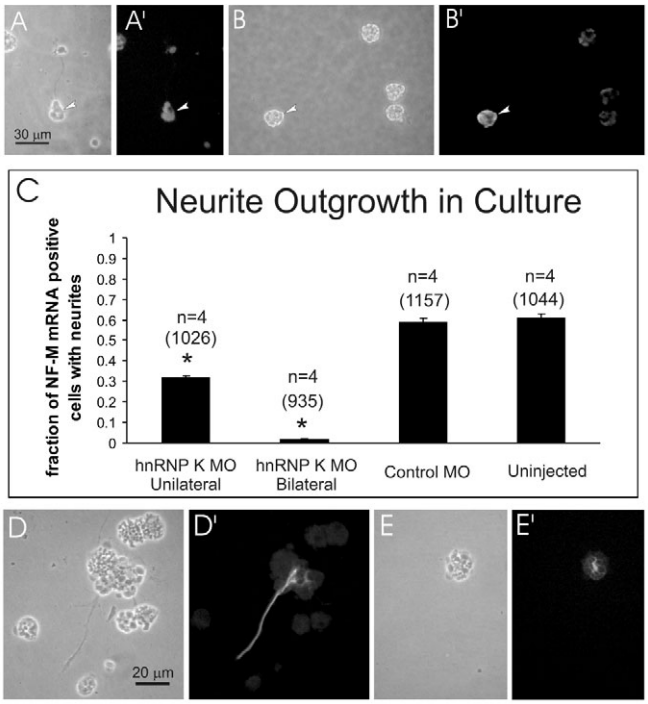

Fig. 7. Effects of hnRNP K knockdown on neurite outgrowth in culture. (**A**,**A′**) Neuron from control MO culture with neurite. (**B**,**B′**) Cells from bilaterally injected *hnRNP K* MO cells lacking neurites. Arrowheads in A and B indicate cells identified as neurons because they were positive for *NF-M* mRNA (by FISH). (**C**) The fraction (±s.d., *n*=4 cultures) of *NF-M* mRNA-positive cells that had neurites. In parentheses are the total number of *NF-M* mRNA-positive cells scored. Asterisks indicate significant variation relative to control MO and uninjected cultures ($P<0.01$, one-way ANOVA). (**D-E′**) Cells in control cultures immunostained for NF-M. Whereas most cells that expressed NF-M had neurites (D), a few did not (E). Scale bars in A and D apply to A-B′ and D-E′, respectively.

RNA-staining that appeared to overlap nuclei (Fig. 8C1,2). When counterstained with DAPI, this staining was clearly seen to overlap with nuclei (Fig. 8D1-4) in both unilaterally and bilaterally injected cultures. Moreover, in bilaterally injected cultures, NF-M protein was absent from virtually all (>98%) *NF-M* RNA positive cells, and these cells had no neurites.

To validate our conclusion that hnRNP K plays an important role in shuttling *NF-M* message effectively from the nucleus, we quantified *NF-M* and *peripherin* RNA from nuclear and cytoplasmic subcellular fractions of bilaterally injected *hnRNP K* MO- and control (stage 29/30) tadpoles. The cytoplasmic/nuclear ratio (determined as ΔC_T from qRT-PCR) was significantly less for *NF-M* mRNA in hnRNP K MO embryos than for either RNA in the other groups ($P<0.01$, one-way ANOVA). Approximately 2.4% (~$2^{-\Delta C_T}$) of the *NF-M* mRNA that was expressed in *hnRNP K* MO embryos was retained in the nucleus, when compared with ~0.03% for other groups, an ~80-fold reduction in the efficiency of nucleocytoplasmic export.

Biochemical assessment of NF-M mRNA translation in hnRNP K knockdown animals

To test whether *NF-M* RNA translation was directly affected, we performed polysomal profiling by sucrose gradient ultracentrifugation. In this assay, more actively translated mRNAs fractionate with polysomes, which lie to the left of the monosomal peak seen in A_{260} plots (Fig. 9). Messages in monosomal or lighter fractions (to the right) are considered translationally silent. In control embryos, *NF-M* mRNA underwent a marked, leftward shift into polysomal fractions between stages 25 (early axonal outgrowth) and 29/30 (the peak of spinal axonal outgrowth), indicating increased translational efficiency. A comparable shift occurs during optic nerve regeneration (Ananthakrishnan et al., 2008), suggesting that this shift in embryos is associated with increased axonal outgrowth. At stage 25, *peripherin* mRNA was already present in polysomal fractions and exhibited a less dramatic shift at stage 29/30, consistent with its being expressed earlier than *NF-M* (Gervasi et al., 2000). In *hnRNP K* MO animals, the leftward shift was virtually eliminated for NF-M mRNA, leaving the mRNA in monosomal and lighter fractions. By stark contrast, the *peripherin* mRNA profile was unaffected, confirming that hnRNP K is not essential for its translation. Such a selective effect indicates that hnRNP K is essential for the translation of only a subset of mRNAs.

Effects of hnRNP K knockdown on other cytoskeletal components

Earlier work in *Xenopus* showing that loss of NF-M attenuates axon elongation without completely abolishing it (Szaro et al., 1991; Lin and Szaro, 1995; Lin and Szaro, 1996; Walker et al., 2001), along with results from knockout mice (Elder et al., 1998), argue that more than a loss of NF-M protein must be at work to account for the loss of axons in hnRNP K knockdown animals. To gain some further insights into this issue, we thus looked at effects in 'neurons' (as identified by peripherin and neuronal tubulin staining) on the three axonal cytoskeletal elements whose synthesis does not require hnRNP K. In bilaterally injected *hnRNP K* MO cultures, peripherin formed twisted filaments and aggregates, and neuronal β-tubulin formed densely packed, ring-like structures, ~2-6 μm in diameter in perikarya (Fig. 10D,F). By contrast, their distributions appeared normal in control MO cultures (Fig. 10C,E). F-actin staining with fluorescent phalloidin was also abnormal. Normally in *Xenopus* cultures, even newly initiated neurites and filopodia stand out with fluorescent phalloidin-staining (Smith et al., 2006), but in bilaterally injected *hnRNP K* MO-cultures, neither filopodia nor neuritic processes were detectable in any cells (Fig. 10B). Instead, F-actin staining was generally circumscribed around the perikaryal periphery, usually with more on one side of the cell than the other, suggesting cells may be polarized despite their failure to initiate neurites. By contrast, neuritic and growth cone lamellipodia and filopodia in control cultures were well stained, with perikaryal hot-spots forming, which is normal (Fig. 10A). Thus, hnRNP K is likely to be important in the post-transcriptional regulation of a set of proteins needed for organizing the cytoarchitecture to form axons.

DISCUSSION

hnRNP K-knockdown by antisense MOs inhibited axon outgrowth, dramatically reducing otherwise robust nerves to the occasional wispy fiber in intact animals and virtually eliminating neuritic outgrowth altogether in culture. This deficiency arose not from inhibiting neuronal differentiation per se, as the expressions of several neuronal markers were unaffected. Instead, it most probably arose from the loss of specific key axonal cytoskeletal proteins whose mRNAs are influenced by hnRNP K, leading to the disrupted cytoarchitectures of essential axonal polymers. Comparing the differential effects on *peripherin* and *NF-M* further indicated at the molecular level that this RNA binding protein in developing *Xenopus* is needed for efficient nucleocytoplasmic shuttling and loading of selective target mRNAs onto polysomes for translation.

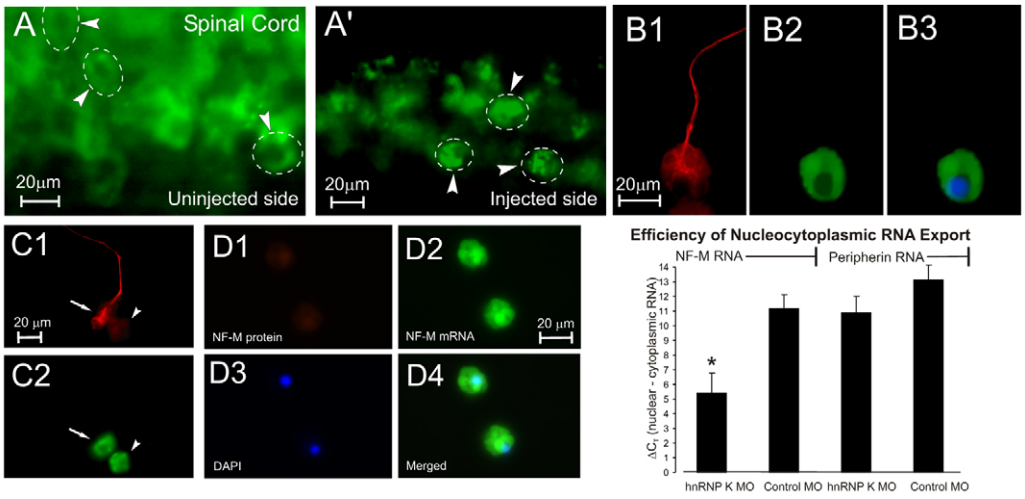

Fig. 8. FISH and immunohistochemistry for NF-M. (**A**,**A′**) *NF-M* FISH of single confocal optical sections from opposite sides of spinal cord or unilaterally injected *hnRNP K* MO1 tadpole (stage 39/40). Broken outlines surround individual neurons. (B1-D4) Cells from dissociated cell culture. (**B1-B3**) Control MO neuron stained for NF-M protein (B1), RNA (B2) and RNA/DAPI merged (B3). (**C1**,**C2**) Adjacent cells from a unilaterally injected hnRNP K MO culture, viewed for NF-M protein (C1) and RNA (C2). Arrow indicates normal staining for both protein and RNA; arrowhead indicates a cell with no protein and FISH pattern typical of hnRNP K MO-injected spinal cord neurons from whole mount. (**D1-D4**) Neurons from a bilaterally injected hnRNP K MO culture stained for protein (D1), RNA (D2), DAPI (D3) and RNA/DAPI merged (D4). Scale bars in B1,C1 and D2 apply to B1-3,C1-2 and D1-4, respectively. Bar graph shows qRT-PCR of nuclear and cytoplasmic fractions for *NF-M* and *peripherin* RNAs from bilaterally injected *hnRNP K* MO and control animals assayed at stage 29/30. ΔC_T, mean (±s.d.) difference in the number of PCR cycles to reach threshold (see text). *ΔC_T was significantly less for *NF-M* RNA in hnRNP K MO embryos than for other groups (P<0.01, one-way ANOVA).

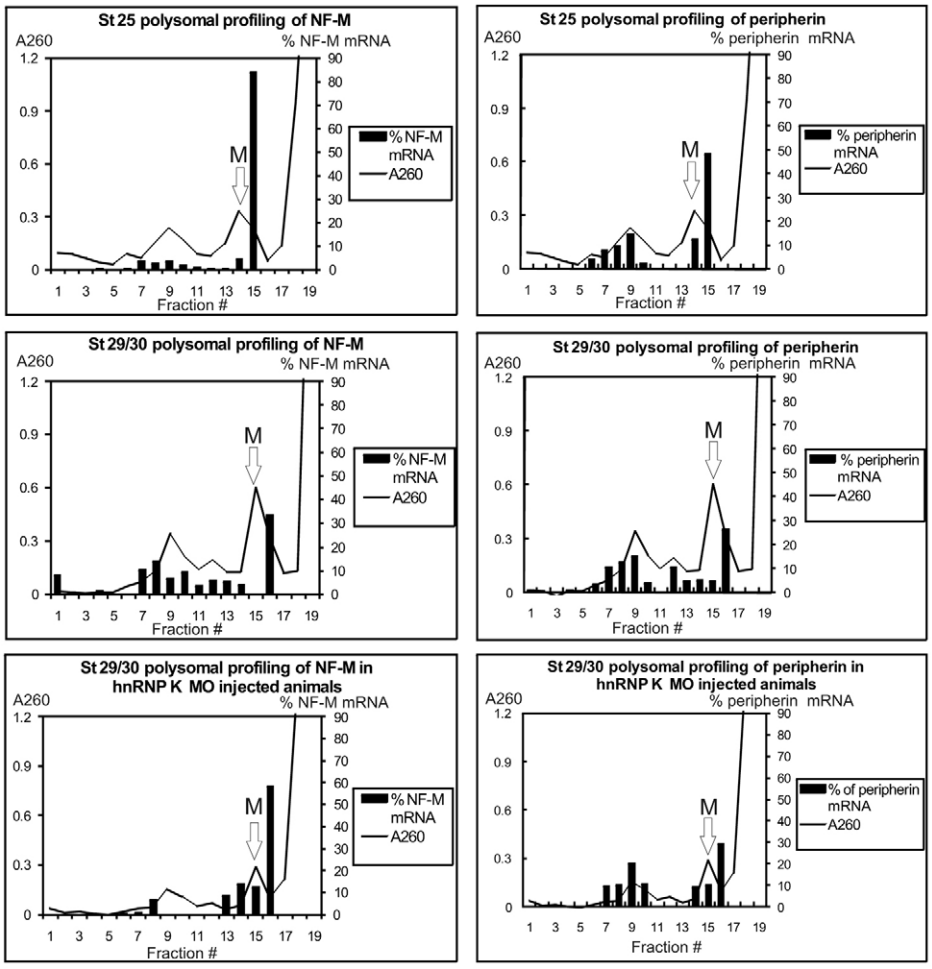

Fig. 9. Polysome profiling of *NF-M* and *peripherin* mRNAs. Black bars indicate the distribution of *NF-M* or *peripherin* mRNA across fractions, represented as a percentage of the total of each respective mRNA in the gradient (right ordinate). The black line depicts A_{260} values (left ordinate) across fractions. 'M' indicates the position of the monosomal peak in the A_{260} trace. (Top four panels) During normal development, *NF-M* (left) and *peripherin* (right) profiles shift from right to left, indicating mRNA moving from poorly translated to efficiently translated fractions. (Bottom two panels) Bilaterally injected *hnRNP K* MO1 embryos processed at stage 29/30. hnRNP K knockdown strongly inhibited the shift into heavier polysomal fractions for *NF-M* but not *peripherin* mRNA.

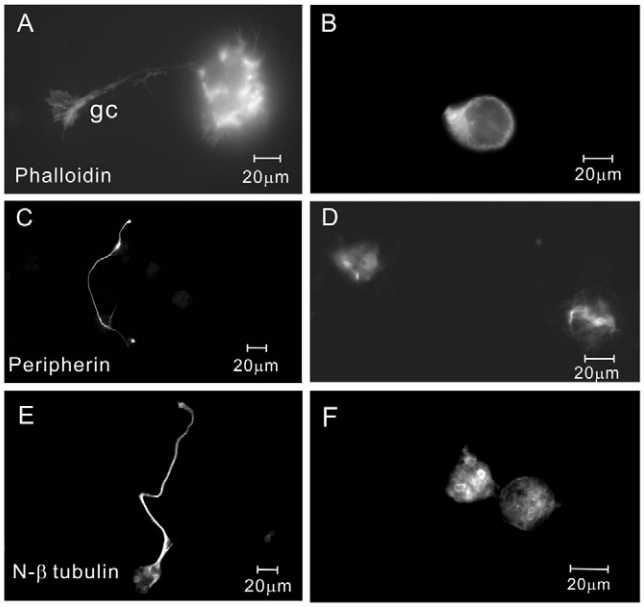

Fig. 10. hnRNP K suppression disrupts cytoskeletal cytoarchitecture. (**A**,**C**,**E**) Bilaterally injected control MO cultures exhibited normal distributions for all three cytoskeletal elements (A, phalloidin-stained F-actin; C, peripherin-immunostained neurofilaments; E, neuron-specific β-tubulin). (**B**,**D**,**F**) The cytoarchitectures of these elements was significantly disrupted in bilaterally injected *hnRNP K* MO cultures. F-actin circumscribed the cell body and was concentrated towards one side (B). Peripherin formed twisted filaments and aggregates (D), and neuronal β-tubulin formed ring-shaped structures (F).

The ubiquitous and early expression of hnRNP K originally led us to anticipate that its knockdown would probably produce an early embryonic lethal. In retrospect, the survival of embryos through early stages of development may have been a fortuitous consequence of the persistence of maternal hnRNP K through gastrula stages, possibly allowing embryos to bypass earlier defects on such processes as cellular proliferation. *hnRNP K* and its *Drosophila* homolog *bancal*, for example, have both been implicated in promoting cell proliferation in neuroblastoma cells and developing appendages (Charroux et al., 1999; Yano et al., 2005). Even so, we saw no evidence of any overall inhibition of cellular proliferation in *Xenopus*, even after hnRNP K expression was thoroughly suppressed: (1) tail formation, which requires cell proliferation, was overtly normal; (2) proliferating-cell-nuclear-antigen (PCNA) was expressed in *hnRNP K* MO-injected descendants (data not shown); and (3) neuronal cell counts (i.e. cells expressing neuronal β-tubulin and *NF-M* mRNA) in dissociated cell culture did not differ significantly between *hnRNP K MO*- and control cultures. Experiments in culture also ruled out any significant cell-autonomous effects on neuronal cell survival, although we can rule out neither secondary trophic effects in the intact animal owing to the loss of axons nor the possibility that hnRNP K plays additional roles at later times.

At the molecular level, hnRNP K knockdown significantly reduced the efficiency of *NF-M* mRNA export from the nucleus and inhibited its loading onto polysomes for translation, leading to suppression of NF-M protein expression. These data, along with its cellular localization, support a role for hnRNP K as a nucleocytoplasmic RNA shuttling protein in *Xenopus*, despite the apparent absence of the KNS nuclear localization signal of human hnRNP K (Siomi et al., 1993; Michael et al., 1997). Shuttling could nonetheless be mediated by alternative sequences in *Xenopus* hnRNP K. For example, it shares an ERK1/2 phosphorylation site with human hnRNP K, which has been implicated in cytosolic localization in HeLa cells (Habelhah et al., 2001). *Drosophila bancal* also exhibits shuttling behavior, despite lacking the KNS motif. Instead, it has an M9 motif, which is known to mediate shuttling of human hnRNPs A1 and A2/B1 (Charroux et al., 1999).

Because hnRNP K has been implicated in multiple, sometimes seemingly contradictory facets of RNA regulation, drawing an explicit connection with any one aspect of mRNA regulation has historically proved difficult (Bomsztyk et al., 1997; Bomsztyk et al., 2004; Ostareck-Lederer et al., 1998). The contemporary view is that hnRNP K serves as the central element of a docking platform that accompanies RNAs from nucleus to cytoplasm, selectively recruiting various elements to the RNA to dictate its fate at any moment (Bomsztyk et al., 2004; Mikula et al., 2006). Our results support such an idea. This raises future questions about how hnRNP K function is regulated. In addition to changes in hnRNP K expression, its actions can be modulated by competition with other RNPs, such as hnRNP E1 (Ostareck et al., 1997; Ostareck-Lederer and Ostareck, 2004) and Hu proteins (Yano et al., 2005), both of which also target *NF-M* mRNA (Antic et al., 1999; Thyagarajan and Szaro, 2004). Such proteins could therefore participate jointly in *NF-M* post-transcriptional regulatory modules. In other instances, hnRNP K actions are regulated by phosphorylation, potentially linking its actions to cell signaling events (Ostareck-Lederer et al., 2002). Our results indicate that the developmental changes in hnRNP K-NF-M RNA interactions seen during postnatal cortical development (Thyagarajan and Szaro, 2008) may underlie regulated changes in NF-M translation.

The most surprising result was the loss of axon outgrowth. The near ubiquitous penetrance of this effect in both intact animals and culture makes it exceedingly unlikely that only a few neuronal subtypes were targeted. Equally unlikely is that axonal loss was caused solely by the loss of NF-M. Instead, the failure of neurites to be initiated, together with the disrupted cytoarchitectures of essential axonal polymers, argue that the axonal defects result from the failure of one or more proteins needed for organizing these polymers to be expressed. These findings raise the intriguing possibility that the translational control of multiple proteins involved in building the axon may be linked through shared elements such as hnRNP K. Our earlier findings that hnRNP K binding to NF-M RNA is developmentally regulated and that NF-M itself is under strong translational control during optic axon regeneration are consistent with hnRNP K being part of such a regulatory module rather than a constitutive facet of NF-M RNA metabolism (Thyagarajan and Szaro, 2004; Thyagarajan and Szaro, 2008; Ananthakrishnan et al., 2008). Future studies to identify the co-factors of hnRNP K, its additional targets during axonogenesis and its mode of regulation should provide the necessary information to distinguish between whether hnRNP K acts as part of a regulatory module influencing several targets via the same mechanism or as one shared element of multiple modules differentially affecting each target separately. Regardless of the outcome of such studies, the current work affirms the importance of post-transcriptional control of selective mRNAs for axon development and identifies hnRNP K as one of the crucial elements.

We thank Drs Amar Thyagarajan and Lakshminarayanan Ananthakrishnan for technical help with the immunoprecipitations and polysome profiling, respectively, and Dr John Schmidt and Kurt Gibbs for editorial comments. The work was supported by NSF IOS 643147 and NYSPHS (New York State Spinal Cord Injury Research Trust) C020940.

Supplementary material

Supplementary material for this article is available at
http://dev.biologists.org/cgi/content/full/135/18/3125/DC1

References

Ananthakrishnan, L., Gervasi, C. and Szaro, B. G. (2008). Dynamic regulation of middle neurofilament (NF-M) RNA pools during optic nerve regeneration. *Neuroscience* **153**, 144-153.

Antic, D., Lu, N. and Keene, J. D. (1999). ELAV tumor antigen, Hel-N1, increases translation of neurofilament M mRNA and induces formation of neurites in teratocarcinoma cells. *Genes Dev.* **13**, 449-461.

Bennett, G. S. and DiLullo, C. (1985). Expression of a neurofilament protein by the precursors of a subpopulation of ventral spinal cord neurons. *Dev. Biol.* **107**, 94-106.

Bomsztyk, K., Van Seuningen, I., Suzuki, H., Denisenko, O. and Ostrowski, J. (1997). Diverse molecular interactions of the hnRNP K protein. *FEBS Lett.* **403**, 113-115.

Bomsztyk, K., Denisenko, O. and Ostrowski, J. (2004). hnRNP K: One protein multiple processes. *BioEssays* **26**, 629-638.

Charroux, B., Angelats, C., Fasano, L., Kerridge, S. and Vola, C. (1999). The levels of the *bancal* product, a *Drosophila* homologue of vertebrate hnRNP K protein, affect cell proliferation and apoptosis in imaginal disc cells. *Mol. Cell. Biol.* **19**, 7846-7856.

Davidson, L. A. and Keller, R. E. (1999). Neural tube closure in *Xenopus laevis* involves medial migration, directed protrusive activity, cell intercalation and convergent extension. *Development* **126**, 4547-4566.

Dent, J. A., Polson, A. G. and Klymkowsky, M. W. (1989). A wholemount immunocytochemical analysis of the expression of the intermediate filament protein vimentin in *Xenopus*. *Development* **105**, 61-74.

Elder, G. A., Friedrich, V. L., Jr, Bosco, P., Kang, C., Giourov, A., Tu, P.-H., Lee, V. M. Y. and Lazzarini, R. A. (1998). Absence of the mid-sized neurofilament subunit decreases axonal calibers, levels of light neurofilament (NF-L) and neurofilament content. *J. Cell Biol.* **141**, 727-739.

Gervasi, C. and Szaro, B. G. (2004). Performing functional studies of *Xenopus laevis* intermediate filament proteins through injection of macromolecules into early embryos. *Methods Cell Biol.* **78**, 673-701.

Gervasi, C., Stewart, C.-B. and Szaro, B. G. (2000). *Xenopus laevis* peripherin (XIF3) is expressed in radial glia and proliferating neural epithelial cells as well as in neurons. *J. Comp. Neurol.* **423**, 512-531.

Gervasi, C., Thyagarajan, A. and Szaro, B. G. (2003). Increased expression of multiple neurofilament mRNAs during regeneration of vertebrate central nervous system axons. *J. Comp. Neurol.* **461**, 262-275.

Gravina, P., Campioni, N., Loreni, F., Pierandrei-Amaldi, P. and Cardinali, B. (2002). Complementary DNA analysis, expression and subcellular localization of *hnRNP E2* gene in *Xenopus laevis*. *Gene* **290**, 193-201.

Habelhah, H., Shah, K., Huang, L., Ostareck-Lederer, A., Burlingame, A. L., Shokat, K. M., Hentze, M. W. and Ronai, Z. (2001). ERK phosphorylation drives cytoplasmic accumulation of hnRNP K and inhibition of mRNA translation. *Nat. Cell Biol.* **3**, 325-330.

Heasman, J. (2002). Morpholino oligos: making sense of antisense? *Dev. Biol.* **15**, 209-214.

Hoperskaya, O. A. (1975). The development of animals homozygous for a mutation causing periodic albinism (a^p) in *Xenopus laevis*. *J. Embryol. Exp. Morphol.* **34**, 253-264.

Iwasaki, T., Koretomo, Y., Fukuda, T., Paronetto, M. P., Sette, C., Fukami, Y. and Sato, K.-I. (2008). Expression, phosphorylation, and mRNA-binding of heterogeneous nuclear ribonucleoprotein K in *Xenopus* oocytes, eggs, and early embryos. *Dev. Growth Differ.* **50**, 23-40.

Keene, J. D. and Tenenbaum, S. A. (2002). Eukaryotic mRNPs may represent posttranscriptional operons. *Mol. Cell* **9**, 1161-1167.

Lin, W. and Szaro, B. G. (1995). Neurofilaments help maintain normal morphologies and support elongation of neurites in *Xenopus laevis* cultured embryonic spinal cord neurons. *J. Neurosci.* **15**, 8331-8344.

Lin, W. and Szaro, B. G. (1996). Effects of intermediate filament disruption on the early development of the peripheral nervous system of *Xenopus laevis*. *Dev. Biol.* **179**, 197-211.

Marcu, A., Bassit, B., Perez, R. and Piñol-Roma, S. (2001). Heterogeneous nuclear ribonucleoprotein complexes from *Xenopus laevis* oocytes and somatic cells. *Int. J. Dev. Biol.* **45**, 743-752.

Meyuhas, O., Bibrerman, Y., Pierandrei-Amaldi, P. and Amaldi, F. (1996). Analysis of polysomal RNA. In *A Laboratory Guide to RNA: Isolation, Analysis, and Synthesis* (ed. P. A. Krieg), pp. 65-81. New York: Wiley-Liss.

Michael, W. M., Eder, P. S. and Dreyfuss, G. (1997). The K nuclear shuttling domain: a novel signal for nuclear import and nuclear export in the hnRNP K protein. *EMBO J.* **16**, 3587-3598.

Mikula, M., Dzwonek, A., Karczmarksi, J., Rubel, T., Dadlez, M., Wyricz, L. S., Bomsztyk, K. and Ostrowski, J. (2006). Landscape of the hnRNP K protein-protein interactome. *Proteomics* **6**, 2395-2406.

Moody, S. A., Miller, V., Spanos, A. and Frankfurter, A. (1996). Developmental expression of a neuron-specific beta-tubulin in frog (*Xenopus laevis*): a marker for growing axons during the embryonic period. *J. Comp. Neurol.* **364**, 219-230.

Moore, M. J. (2005). From birth to death: the complex lives of eukaryotic mRNAs. *Science* **309**, 1514-1518.

Nordlander, R. H. (1989). HNK-1 marks earliest axonal outgrowth in *Xenopus*. *Dev. Brain Res.* **50**, 147-153.

Ostareck, D. H., Ostareck-Lederer, A., Wilm, M., Thiele, B. J., Mann, M. and Hentze, M. W. (1997). mRNA silencing in erythroid differentiation: hnRNP K and hnRNP E1 regulate 15-lipoxygenase translation from the 3′ end. *Cell* **89**, 597-606.

Ostareck-Lederer, A. and Ostareck, D. H. (2004). Control of mRNA translation and stability in haematopoietic cells: the function of hnRNPs K and E1/E2. *Biol. Cell* **96**, 407-411.

Ostareck-Lederer, A., Ostareck, D. H. and Hentze, M. W. (1998). Cytoplasmic regulatory functions of the KH-domain proteins hnRNPs K and E1/E2. *Trends Biochem. Sci.* **23**, 409-411.

Ostareck-Lederer, A., Ostareck, D. H., Cans, C., Neubauer, G., Bomsztyk, K., Superti-Furga, G. and Hentze, M. W. (2002). c-Src-mediated phosphorylation of hnRNP K drives translational activation of specifically silenced mRNAs. *Mol. Cell. Biol.* **22**, 4535-4543.

Perrone-Bizzozero, N. L. and Bolognani, F. (2002). Role of HuD and other RNA-binding proteins in neural development and plasticity. *J. Neurosci. Res.* **68**, 121-126.

Piñol-Roma, S. and Dreyfuss, G. (1992). Shuttling of pre-mRNA binding proteins between nucleus and cytoplasm. *Nature* **355**, 730-732.

Shain, D. H. and Zuber, M. X. (1996). Sodium dodecyl sulfate (SDS)-based whole-mount in situ hybridization of *Xenopus laevis* embryos. *J. Biochem. Biophys. Meth.* **31**, 185-188.

Si, K., Giustetto, M., Etkin, A., Hsu, R., Janisiewicz, A. M., Miniaci, M. C., Kim, J.-H., Zhu, H. and Kandel, E. R. (2003). A neuronal isoform of CPEB regulates local protein synthesis and stabilizes synapse-specific long-term facilitation in *Aplysia*. *Cell* **115**, 893-904.

Siomi, H., Matunis, M. J., Michael, W. M. and Dreyfuss, G. (1993). The pre-mRNA binding K protein contains a novel evolutionarily conserved motif. *Nucleic Acids Res.* **21**, 1193-1198.

Smith, A., Gervasi, C. and Szaro, B. G. (2006). Neurofilament content is correlated with branch length in developing collateral branches of *Xenopus* spinal cord neurons. *Neurosci. Lett.* **403**, 283-287.

Szaro, B. G. and Gainer, H. (1988). Identities, antigenic determinants, and topographic distributions of neurofilament proteins in the nervous systems of adult frogs and tadpoles of *Xenopus laevis*. *J. Comp. Neurol.* **273**, 344-358.

Szaro, B. G., Lee, V. M. Y. and Gainer, H. (1989). Spatial and temporal expression of phosphorylated and non-phosphorylated forms of neurofilament proteins in the developing nervous system of *Xenopus laevis*. *Dev. Brain Res.* **48**, 87-103.

Szaro, B. G., Grant, P., Lee, V. M. Y. and Gainer, H. (1991). Inhibition of axonal development after injection of neurofilament antibodies into a *Xenopus laevis* embryo. *J. Comp. Neurol.* **308**, 576-585.

Tabti, N. and Poo, M.-M. (1991). Culturing spinal neurons and muscle cells from *Xenopus* embryos. In *Culturing Nerve Cells* (ed. G. Banker and K. Goslin), pp. 137-154. Cambridge: MIT Press.

Tenenbaum, S. A., Lager, P. J., Carson, C. C. and Keene, J. D. (2002). Ribonomics: identifying mRNA subsets in mRNP complexes using antibodies to RNA-binding proteins and genomic arrays. *Methods* **26**, 191-198.

Thyagarajan, A. and Szaro, B. G. (2004). Phylogenetically conserved binding of specific KH domain proteins to the 3′ untranslated region of the vertebrate middle neurofilament mRNA. *J. Biol. Chem.* **279**, 49680-49688.

Thyagarajan, A. and Szaro, B. G. (2008). Dynamic endogenous association of neurofilament mRNAs with K-homology domain ribonucleoproteins in developing cerebral cortex. *Brain Res.* **1189**, 33-42.

Undamatla, J. and Szaro, B. G. (2001). Differential expression and localization of neuronal intermediate filament proteins within newly developing neurites in dissociated cultures of *Xenopus laevis* embryonic spinal cord. *Cell Motil. Cytoskel.* **49**, 16-32.

Walker, K. L., Yoo, H.-K., Undamatla, J. and Szaro, B. G. (2001). Loss of neurofilaments alters axonal growth dynamics. *J. Neurosci.* **21**, 9655-9666.

Wetzel, D. M., Lee, V. M. Y. and Erulkar, S. D. (1989). Long term cultures of neurons from adult frog brain express GABA and glutamate-activated channels. *J. Neurobiol.* **20**, 255-270.

Yano, M., Okano, H. J. and Okano, H. (2005). Involvement of Hu and heterogeneous nuclear ribonucleoprotein K in neuronal differentiation through p21 mRNA post-transcriptional regulation. *J. Biol. Chem.* **280**, 12690-12699.

Yao, J., Sasaki, Y., Wen, Z., Bassell, G. J. and Zheng, J. Q. (2006). An essential role for beta-actin mRNA localization and translation in Ca^{2+}-dependent growth cone guidance. *Nat. Neurosci.* **9**, 1265-1273.

Zhao, Y. and Szaro, B. G. (1994). The return of phosphorylated and nonphosphorylated epitopes of neurofilament proteins to the regenerating optic nerve of *Xenopus laevis*. *J. Comp. Neurol.* **343**, 158-172.